A Leaner Carrier for the New 5G Air Interface

Kilian Roth*, Cecilia Carbonelli§, Michael Faerber§, Josef A. Nossek*

*Institute for Circuit Theory and Signal Processing, Technical University Munich,
Munich, Germany, kilian.roth@tum.de, josef.a.nossek@tum.de

§Standards and Advanced Technology, Intel Mobile Communications, Neubiberg, Germany
cecilia.carbonelli@ieee.org, michael.faerber@intel.com

***Abstract*—This paper studies the physical layer performance of a lean carrier with reduced reference symbols and reduced control channel overhead as a possible candidate for a new 5G air interface. Specifically, we will show that, with minor modifications and optimizations, competitive link level performance can be achieved even in extreme use case scenarios using synchronization and channel estimation algorithms already employed in LTE-A. Further, we propose a set of enhancements to the broadcast channel and to the common search space configurations to fully dispense with cell specific reference symbols and legacy control channels.**

Keywords—Lean carrier; 5G air interface; control channels; broadcast channel; synchronization; channel estimation.

I. INTRODUCTION

Reducing system overhead to improve system efficiency is a design goal for new air interface concepts, and for enhancements in existing ones. The idea of a new, leaner LTE carrier with a minimized set of cell specific reference symbols (CRS) was first discussed in 3GPP Release 12 to improve spectral efficiency, to reduce power consumption at Base Stations (BS), and to mitigate intercell interference [1, 2]. Most of the activities focused on small cell enhancements and highlighted the advantages of employing a 'leaner carrier type' (LCT) (aka 'new carrier type', NCT) for low power nodes. The goal here was network densification [3, 4], a use case model widely adopted today to describe 5G network layouts.

Although the LCT discussion in 3GPP has been recently suspended due to a large number of open topics and non-converging system level simulation results [5, 6], the need for a leaner carrier remains unchanged in the framework of a new air interface for the next generation (5G) cellular technology [7].

In this manuscript, using the new frame structure proposed in 3GPP [5] for the LCT, we provide a very comprehensive link level performance evaluation of those baseband processing elements which are most sensitive to the reduction of the number of reference symbols. These include time and frequency synchronization algorithms as well as the Physical Broadcast Channel (PBCH) processing. For the PBCH a new channel estimation scheme based on the Primary and Secondary Synchronization Sequence (PSS/SSS) is introduced and the performance is compared to a CRS based channel estimate. We will prove the feasibility of LCT with state-of-the art schemes and suggest improvements and optimizations.

Another important goal of our work it to investigate the open standardization aspects and propose a viable solution to enable leaner and more flexible carriers. The working assumption of the paper is that also future 5G air interfaces will have a similar control and transport channel structure as LTE. To this end, we note that the enhanced Physical Downlink Control Channel (ePDCCH) introduced in the 3GPP Release 11 [8] is still in many respects an add-on rather than a natively included feature since it relies on the coexistence with the legacy Physical Downlink Control Channel (PDCCH). Specifically, in the current specification the ePDCCH is configured through Radio Resource Control (RRC) messages which can be accessed in the Physical Downlink shared Channel (PDSCH) only after having decoded the legacy PDCCH Common Search Space (CSS). Also, only a User Equipment Specific Search Space (UESS) is defined for ePDCCH. Finally, the Uplink Hybrid Automatic Repeat Request (HARQ) indication is currently mapped on the legacy Physical HARQ Indicator Channel (PHICH). It is thus clear that changes to the current standard are required to be able to fully combine the ePDCCH with a standalone and non-backward compatible carrier in an evolved LTE-A concept. A way forward to address these remaining issues will be provided in this paper.

The paper is organized as follow. Section II introduces our system model and frame structure. Section III discusses frequency and time synchronization performance of LCT compared to the existing LTE-A Transmission Mode 9 (TM9). PBCH decoding performance are presented in Section IV, while further enhancements to ePDCCH in combination with LCT are proposed in Section V. Conclusions are drawn in Section VI.

II. SYSTEM MODEL

Figure 1 shows the LCT frame structure employed in this paper [5]. The CRS are transmitted in subframe 0 and 5 from one antenna port while the transmission of data and control information is based on the Demodulation Reference Symbols (DMRS) [8] which are only present in those Physical Resource Blocks (PRB) where the User Equipment (UE) is allocated. The ePDCCH entirely replaces the legacy PDCCH whereas the synchronization symbols and the broadcast channel remain at the same positions.

Since many different aspects of the LCT where not agreed in the 3GPP standardization, a number of plausible assumptions

978-1-4799-8088-8/15/$31.00 ©2015 IEEE

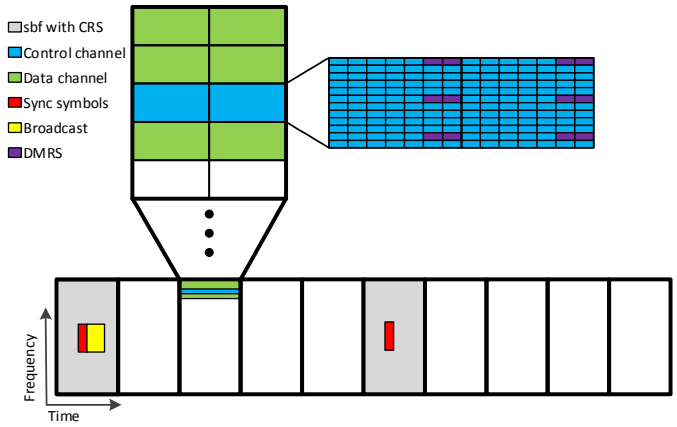

Fig. 1. LCT frame structure

need to be made to be able to simulate throughput performance. Specifically, the DMRS are the same as the DMRS used in standard LTE TM9 and ePDCCH contains all necessary control information (see Section V). Further, a receiver with two antennas is assumed and a normal cyclic prefix (CP) is used.

III. Frequency and Time Synchronization

In the following we discuss frequency and time synchronization for the LCT. While the initial coarse synchronization can still be carried out in the cell search phase resorting to the existing LTE synchronization symbols, the fine tracking of the time and frequency residual offset requires more attention. In fact, synchronization algorithms have to completely rely on a reduced set of CRS and, where needed, on the DMRS available in the PRBs where the UE is scheduled.

A. Frequency Offset Tracking

In OFDM based systems Doppler shifts and oscillator instabilities can cause a carrier frequency offset which destroys the orthogonality between subcarriers and severely degrades the system performance. In addition, a time dependent phase offset is introduced, which affects the channel estimation performance. The goal of fine offset frequency tracking is to continuously estimate and compensate the residual time-varying frequency shift after the initial acquisition phase.

Keeping in mind the frame structure in Figure 1, we can base our estimates on the correlation between CRS for those subframes where CRS are present (i.e. subframe 0 and 5) across the entire system bandwidth (Figure 2). Alternatively, one could calculate the correlation between DMRS belonging to the same subframe for those PRBs where the UE is scheduled. The former is a worst case choice and will be used in our simulations.

Specifically, we adopt a frequency domain approach [9] and compute the offset normalized to the carrier spacing as:

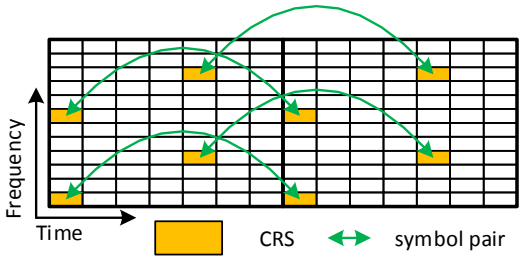

Fig. 2. CRS pairs for frequency offset estimation (subframe 0 and 5)

$$\varepsilon_f = \frac{\angle\left(\sum D_{k,l} D^*_{k,l+L}\right)}{-2\pi L(1+N_g/N)} \tag{1}$$

where

$$D_{k,l} = R_{k,l} X^*_{k,l} = e^{j\phi_l(\varepsilon_f)} H_{k,l} + W_{k,l} X^*_{k,l} \tag{2}$$

are the demodulated reference symbols, $R_{k,l}$ and $X_{k,l}$, are the received and transmit symbols, respectively, while $H_{k,l}$ and $W_{k,l}$ denote the channel frequency response and the noise at the generic subcarrier k and OFDM symbol l. The frequency offset leads to a phase offset equal to

$$\phi_l(\varepsilon_f) = 2\pi l \varepsilon_f (N + N_g)/N \tag{3}$$

on OFDM symbol l. The OFDM FFT size and the number of samples of the cyclic prefix are represented by N and N_g. Finally, L is the distance between OFDM symbols carrying CRS (or DMRS). The summation in (1) goes over all possible reference symbol pairs with the same distance L.

Once the offset is estimated we can use a conventional IIR or FIR filter to track its value over time, as discussed in the results section. We also observe that the offset can be compensated prior to Fast-Fourier Transform (FFT) or after. In our simulations we adopted a pre-FFT approach due to slightly better noise performance [10].

B. Time Offset Tracking

Time synchronization is a critical problem in every communications system. As long as the CP of the OFDM system is longer than the channel impulse response, the position of the FFT window includes samples from only one OFDM block and no inter-block interference (IBI) is generated. The time offset would then only result in a phase-shift, which is later removed by the channel estimation.

In this paragraph we assume perfect frequency synchronization and an initial coarse time acquisition so that the remaining time error is expected to be in the range of the cyclic prefix. As for the frequency case, we rely on the correlation products between CRS for those subframes where CRS are present (i.e. subframe 0 and 5) across the entire

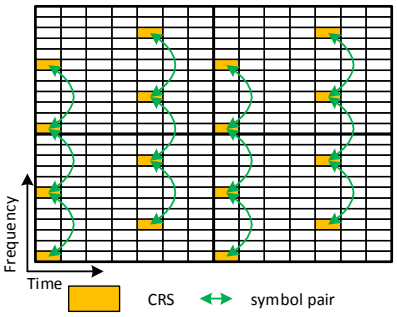

Fig. 3. CRS pairs for time offset estimation (subframe 0 and 5)

system bandwidth (Figure 3). Alternatively, one could calculate the correlation between DMRS belonging to the same subframe for those PRBs where the UE is scheduled. The former is a worst case approach and will be used in our simulations.

Again, we work in the frequency domain [9] and compute the offset normalized by the sampling time as:

$$\varepsilon_t = \frac{\angle\left(\sum D_{k,l} D_{k+K,l}\right)}{2\pi K / N} \tag{4}$$

where

$$D_{k,l} = R_{k,l} X^*_{k,l} = e^{j\phi_k(\varepsilon_t)} H_{k,l} + W_{k,l} X^*_{k,l} \tag{5}$$

are the demodulated reference symbols presented in (2) with the only difference that the time offset results in a phase rotation on subcarrier k. The phase rotation is defined as:

$$\phi_k(\varepsilon_t) = -2\pi k \varepsilon_t / N \tag{6}$$

In (4) K is the distance between the subcarriers used in the correlation pair for the calculation of the offset. Also, the summation in (4) takes into account all possible correlation pairs with subcarrier distance equal to K. Similarly to the frequency case, once the offset is estimated we can use a conventional IIR or FIR filter to track its value over time, as discussed in the results section. We also observe that the offset can be compensated prior to Fast-Fourier Transform (FFT) or after. In our simulations we adopted a pre-FFT approach due to its lower complexity [10].

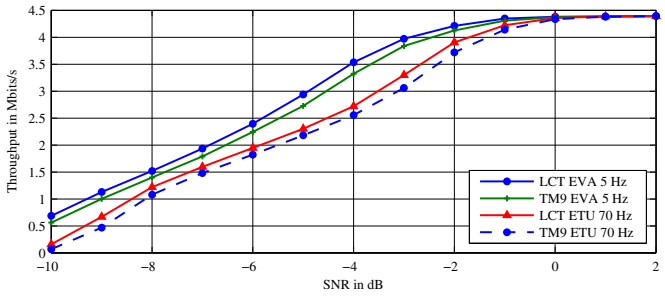

Fig. 4. Throughput comparison of LCT and TM9 in the presence of frequency offset

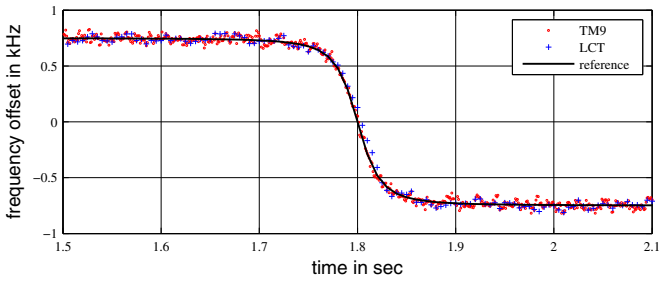

Fig. 5. HST estimated frequency offset

C. Results

In Figure 4 we show the throughput performance of the frequency tracking approach described above. We assume a 10 MHz bandwidth, Modulation and Coding Scheme (MCS) = 5 (QPSK with code rate 0.3), 2 transmit (TX) and 2 receive (RX) antennas and a fixed frequency offset of 200 Hz. LCT and LTE-A TM9 are compared for the Extended Vehicular A (EVA) and Extended Typical Urban (ETU) channel [11] with an additional Doppler shift of 5Hz and 70Hz and one spatial multiplexing layer. An IIR filter of the 1st order is used for tracking. The control overhead for TM9 was fixed to 2 OFDM symbols, while the ePDCCH for the LCT consisted of 4 PRBs. Singular Value Decomposition based precoding has been applied to the transmitted data and DMRS symbols in the case of LCT and TM9. Since the DMRS are only transmitted in those PRB pairs containing control information or data, the tracking results presented here only utilize CRS for the offset estimation to represent the worst possible tracking performance. The slightly superior performance of LCT is due to the reduced reference overhead resulting in a higher code rate, while similar frequency offset estimation accuracy to the TM9 case has been observed.

Another scenario where the frequency tracking algorithm is significantly challenged is the High Speed Train (HST) case [11]. Here a train which is traveling at a speed of 300 km/h is modelled and the BS is positioned 2 meters from the train track. At the time the train passes by the BS the Doppler shift changes from a large positive value (750 Hz) to a large negative value (-750 Hz) in a relatively short time. The time dependency of the Doppler frequency shift is shown in Figure 5. Except for the Doppler shift, the channel is modelled as a full rank AWGN channel. The estimated offset for both LCT and TM is shown in Figure 5. Again, both setups achieve similar performance and are very close to the reference curve.

As far as the time tracking is concerned, we show in Figure 6 the throughput performance obtained for LCT and TM9 for two different channel profiles, ETU 185 Hz and EVA 5Hz. We assume a 15 MHz bandwidth, MCS = 5 (QPSK with coding rate 0.3), 2 TX and 2 RX antennas and a fixed time offset of -1μs. An IIR filter of the 1st order is used for tracking.

Again, although the time estimation accuracy is comparable, a slight better performance is observed for the LCT due to the availability of more channel bits. More details

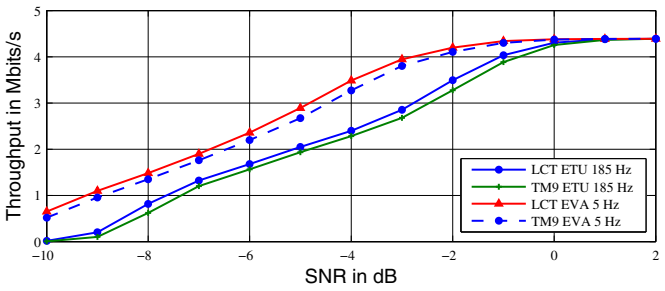

Fig. 6. Throughput comparison of LCT and TM in the presence of time offset

on the impact of the power delay profile on the residual time estimation bias of the algorithm employed for these simulations are provided in [10].

Although the above results show satisfactory performance when the existing LTE reference symbol structure is re-used and extended, we note that the introduction of new and optimized pilot patterns might bring additional gain. This analysis is beyond the scope of the paper.

IV. Broadcast Channel

After searching for the Primary and Secondary Synchronization Sequences (PSS and SSS) and obtaining information about cell identity (cell-ID), duplexing mode and CP length, the UE has to decode the Master Information Block (MIB) transmitted on the broadcast channel and gain knowledge on the system bandwidth and other parameters needed for initial access to the cell. In this paragraph we are going to evaluate the performance of the broadcast channel decoding procedure when a reduced set of CRS is available.

In LTE/LTE-A the PBCH occupies the 72 center subcarriers of 4 consecutive OFDM symbols in subframe 0. The coded and rate matched bits are segmented into 4 blocks, each block being separately decodable. In standard LTE the PBCH can be transmitted via 1, 2 or 4 antenna ports depending on how many ports are used for the transmission of CRS. In the case of 2 or 4 antennas an Alamouti based Space Frequency Block Code (SFBC) Transmit-Diversity (Tx-Div) scheme is applied. Only QPSK modulation is used.

Before decoding the PBCH the UE does not know how many CRS antenna ports are used and blind decoding needs to be applied where all hypothesis are tested. This discovery is further facilitated by masking the Cyclic Redundancy Check (CRC) on each MIB with a sequence representing the number of transmit antenna ports. Also, those symbols where CRS could be placed in the worst case of 4 TX antennas are reserved and cannot be used for data transmission. In LCT only one CRS TX antenna is used. Therefore it is possible to utilize the remaining unused symbols for transmitting the PBCH. One of these PBCH transmission blocks is shown in Figure 7. The left time-frequency grid represents the standard LTE subframe. The right grid represents the LCT subframe where additional REs are used for the PBCH transmission. While in the standard LTE there are 1920 encoded bits, in the case of LCT we have 288 additional channel encoded bits.

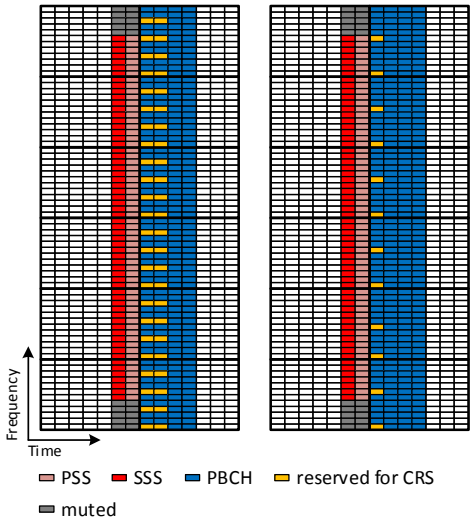

Fig. 7. Broadcast channel frame structure

These bits can be used to either decrease the code rate from 0.0208 to 0.0181 or to add 6 information bits and keep the same code rate.

Further, as shown in Figure 7 the PSS/SSS are placed exactly before the broadcast channel. Since these symbols are known, our idea is to use them to enable an Alamouti Tx-Div scheme also for the LCT case (which usually relies on 1 TX antenna only) after obtaining a proper channel estimate, and compare it to the standardized 2 TX LTE in terms of Block Error Rate (BLER), as discussed in Sections IV-A and IV-B.

A. Proposed Channel Estimation

As far as channel estimation is concerned, for the LCT in the 2TX scenario we propose to apply the MMSE approach in [12] to both the CRS and PSS/SSS. Perfect knowledge of the second order channel statistics is assumed.

For the case of PSS/SSS based channel estimation, the PSS/SSS symbols are filtered in frequency direction and averaged over both OFDM symbols 5 and 6 in time domain. The length of the frequency filter is fixed so as to achieve the same computational complexity of the CRS based approach. This estimate is then used for all OFDM symbols containing the PBCH. Since the PBCH region is 5 subcarriers wider than the PSS/SSS area, the channel estimate for the edge subcarriers needs to be extrapolated leading to performance degradation. Still, it can be shown [10] that the channel estimation accuracy achieved resorting to the PSS/SSS is higher than in the CRS case, for the same computational complexity, due to the possibility to use longer filters and a denser pilot spacing.

B. Results

In Figure 8 we compare: *i)* for the 1TX antenna case, the standard CRS based and the proposed PSS/SSS based approach; *ii)* for the 2 TX antenna case, the standard CRS based and the proposed mixed CRS-PSS/SSS based approach. We assume low antenna correlation and an ETU 70Hz channel.

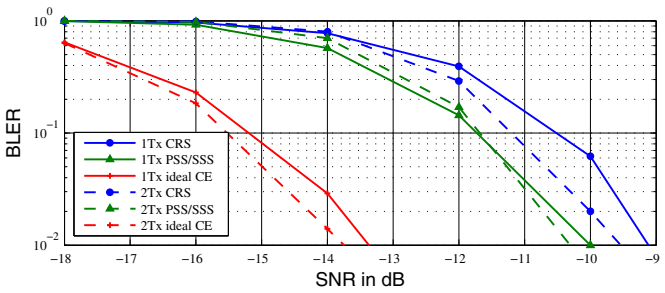

Fig. 8. PBCH BLER performance for ETU 70Hz, low correlation

It can be seen that, in the 1TX antenna case, the channel estimate based on the PSS/SSS symbols offers better BLER performance than the CRS based one, particularly in the presence of highly frequency selective channels. In the 2TX antenna case this gain is more contained since the BLER performance is dominated by the antenna where the conventional CRS approach is applied. Still, for LCT it is possible to reuse the PSS/SSS symbols for channel estimation and achieve a better performance compared to a conventional CRS based channel estimate without additional overhead.

V. Further Air Interface Enhancements

We now discuss the remaining necessary steps to enable a fully standalone leaner carrier. This can be seen as a way forward for further LTE-A evolution or for a non-compatible 5G air interface solution. The required steps mostly involve the ePDCCH channel (or its 5G equivalent) and its configuration. In fact, there are currently no standardized solutions to configure the ePDCCH channel, to support CSS and to signal the Uplink HARQ ACK/NACK in the absence of legacy control channels (and thus of higher layer/RRC signaling) and in the context of a leaner carrier type. Discussion on this serious open issue is ongoing in 3GPP, but no solutions have been proposed or agreed yet. The current LTE working assumption is that ePDCCH and PDCCH are always both configured and the latter can be used to finally locate the former and, at the same time, to identify the common search space, while the Uplink HARQ indication is mapped on the Physical HARQ Indicator Channel (PHICH).

Our proposal for a standalone ePDCCH (S-ePDCCH) offers a simple and intuitive solution to the identified problem(s) and enables a more flexible implementation of the control channels. Specifically, we propose to use the PBCH to configure the S-ePDCCH and thus allow the UE to locate both CSS and UESS, depending on the specific UE state, in the given subframe. To this end, for example, one could use the bits that are still available in the PBCH MIB to address the S-ePDCCH PRB pairs. Additional configuration parameters could be signaled by introducing new CRC mask sequences. Alternatively, the S-ePDCCH PRB pairs could occupy fixed positions (with an additional cell ID dependent frequency shift). In this case, no explicit information needs to be carried in the PBCH.

Finally, to be able to dispense with the legacy control channel we need to make sure that the Uplink HARQ indicator is mapped to the Common Search Space or to the UE Specific Search Space of the newly defined S-ePDCCH. Since the physical downlink control channel information is protected by a channel code (which is not the case for the PHICH), the repetition code used for PHICH is no longer necessary and 1 bit is sufficient. There are multiple options to pack both 3-bit ACK/NACK states ‘000’ or ‘111’ as a single bit for example in the CSS Downlink Control Indicator formats 1A and 1C which already carry the HARQ process number as well as the ePDCCH-specific HARQ-ACK offset.

VI. Conclusions

In this paper we demonstrated the feasibility of a leaner OFDM carrier type in the framework of a new air interface candidate for 5G or for a non-backward compatible LTE-A evolution. Extending the concept initially standardized within the LTE Release 11 and making some realistic assumptions on the aspects not yet covered by 3GPP, we provided an overview of the link level performance that can be achieved by the LCT using simple physical layer algorithms. We showed that in many scenarios small to significant gains are observed over the conventional LTE-A system. Future enhancements to reduce the control channel overhead and make the LCT fully flexible are also proposed and discussed.

Acknowledgement

The authors would like to thank their colleagues at Intel Mobile Communications, Stefan Fechtel and Michael Horvat, for fruitful discussions on the topic treated in this paper.

References

[1] C. Hoymann, D. Larsson, H. Koorapaty, and J-F. Cheng, “A lean carrier for LTE”, Communications Magazine, IEEE, 51(2), Feb 2013.

[2] D. Astely, E. Dahlman, G. Fodor, S. Parkvall, J. Sachs, "LTE release 12 and beyond”, IEEE Communications Magazine, 51 (7), 2013.

[3] T. Nakamura, S. Nagata, A. Benjebbour, Y. Kishiyama, Shen X. Tang Hai; Yang Ning; Li Nan, "Trends in small cell enhancements in LTE advanced”, IEEE Communications Magazine, 51(2), 2013.

[4] H. Ishii, Y. Kishiyama, H. Takahashi, “A novel architecture for LTE-B: C-plane/U-plane split and Phantom Cell concept”, IEEE Globecom Workshops, 2012.

[5] Ericsson, ST-Ericsson, Huawei, Hi-Silicon, “Summary of Performance Evaluation Results for Standalone NCT”, 3GPP R1-133976, August 2013.

[6] Ericsson, ST-Ericsson, Huawei, Hi-Silicon, “Merge of evaluation assumptions for small cell on/off and S-NCT”, 3GPP TS R1-132849, May 2013.

[7] Woon Hau Chin ; Zhong Fan ; R. Haines, "Emerging technologies and research challenges for 5G wireless networks”, IEEE Wireless Communications, 21 (2), 2014.

[8] 3GPP, Evolved Universal Terrestrial Radio Access (E-UTRA); Physical channels and modulation TS 36.211, Mar. 2014.

[9] M. Morelli, C. C. J. Kuo, M. O. Pun, “Synchronization techniques for orthogonal frequency division multiple access (OFDMA): A tutorial review”, in Proc. IEEE, Vol. 95, No. 7, pp. 1394-1427, July 2007.

[10] K. Roth, “LTE Lean Carrier Type (LCT)” (Master Thesis), Technical University Munich, June 2014.

[11] 3GPP, Evolved Universal Terrestrial Radio Access (E-UTRA); User Equipment (UE) radiotransmission and reception. TS 36.101, Mar. 2013.

[12] P. Hoeher, S. Kaiser, P. Robertson, “Pilot-Symbol-Aided Channel Estimation in Time and Frequency”, In Proc. ICASSP'97, Volume 3, pp. 1845-1848, Munich, April 1997.